

# RSC Advances



This is an *Accepted Manuscript*, which has been through the Royal Society of Chemistry peer review process and has been accepted for publication.

*Accepted Manuscripts* are published online shortly after acceptance, before technical editing, formatting and proof reading. Using this free service, authors can make their results available to the community, in citable form, before we publish the edited article. This *Accepted Manuscript* will be replaced by the edited, formatted and paginated article as soon as this is available.

You can find more information about *Accepted Manuscripts* in the [Information for Authors](#).

Please note that technical editing may introduce minor changes to the text and/or graphics, which may alter content. The journal's standard [Terms & Conditions](#) and the [Ethical guidelines](#) still apply. In no event shall the Royal Society of Chemistry be held responsible for any errors or omissions in this *Accepted Manuscript* or any consequences arising from the use of any information it contains.

## Graphical Abstract

### CuO Nanorods: A potential and Efficient Adsorbent in Water Purification

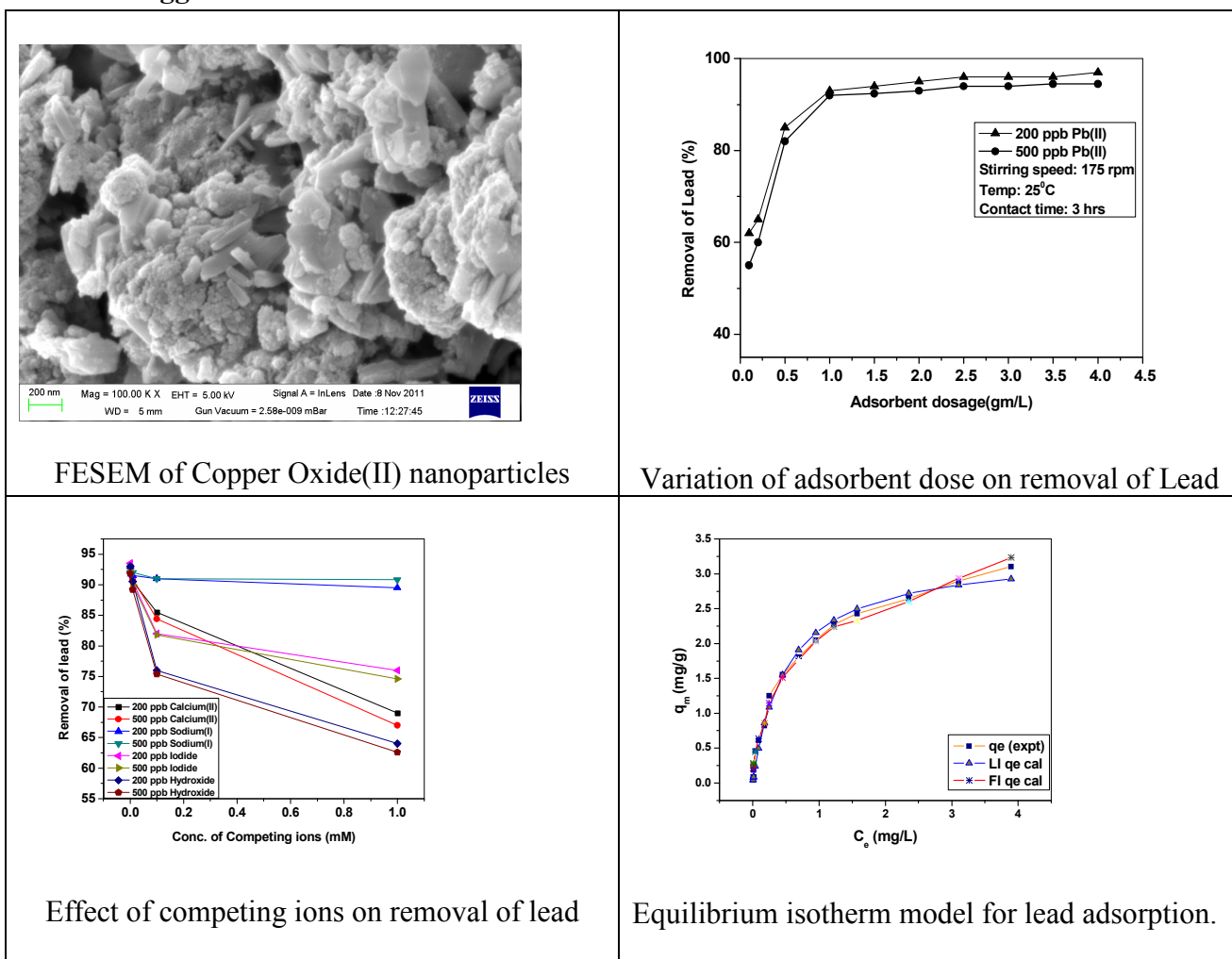
Prasanta Kumar Raul<sup>a\*</sup>, Samarpita Senapati<sup>b</sup>, Ashish K Sahoo<sup>b</sup>, Iohborlang M. Umlong<sup>a</sup>, Rashmi R Devi<sup>a</sup>, Ashim Jyoti Thakur<sup>c</sup>, Vijay Veer<sup>a</sup>

<sup>a</sup> Defence Research Laboratory, Post Bag No. 2, Tezpur- 784 001, Assam, India.

<sup>b</sup> Department of Chemistry, Indian Institute of Technology Kharagpur, Kharagpur-721302, India

<sup>c</sup> Department of Chemical Sciences, Tezpur University, Napaam, Tezpur-784028, Assam, India

**CuO nanorods can remove Pb(II) from aqueous solution with maximum sorption capacity of 3.31 mgg<sup>-1</sup> at 298K.**



## CuO Nanorods: A potential and Efficient Adsorbent in Water Purification

Prasanta Kumar Raul<sup>a\*</sup>, Samarpita Senapati<sup>b</sup>, Ashish K Sahoo<sup>b</sup>, Iohborlang M. Umlong<sup>a</sup>, Rashmi R Devi<sup>a</sup>, Ashim Jyoti Thakur<sup>c</sup>, Vijay Veer<sup>a</sup>

<sup>a</sup> Defence Research Laboratory, Post Bag No. 2, Tezpur- 784 001, Assam, India.

<sup>b</sup> Department of Chemistry, Indian Institute of Technology Kharagpur, Kharagpur-721302, India

<sup>c</sup> Department of Chemical Sciences, Tezpur University, Napaam, Tezpur-784028, Assam, India.

\*Corresponding author: Prasanta Kumar Raul; Fax No.: +91 3712258534;

Email id: [prasanta.drdo@gmail.com](mailto:prasanta.drdo@gmail.com)

Abstract:

The present work deals with a simple in-situ soft chemical synthesis of nanoscale copper (II) oxide, its characterization and study of adsorption and desorption behaviors of Pb(II) on nano CuO. The nanoparticles are characterized by XRD, FESEM, TEM and BET surface area analyzer. Electron microscopy image clearly reveals rod like morphology of rhombohedral CuO, with average diameter  $\sim 5$  nm and length extending up to 50 nm. BET shows average surface area of the nanorods  $\sim 52.57 \text{ m}^2\text{g}^{-1}$ . In adsorption study, the influence of operational conditions such as contact time, initial concentration of Pb(II), initial pH of solution and temperature on the adsorption of Pb(II) has also been examined. Studies also reveal that the Pb(II) uptake onto CuO is a fast process and  $>70\%$  of the uptake occurred within the first 10 min contact time and attained  $>92\%$  in 60 min. The maximum sorption capacity of Pb(II) is  $3.31 \text{ mgg}^{-1}$  at 298K. The +ve  $\Delta S^0$  value and +ve  $\Delta H^0$  value of  $37.77 \text{ kJ/mol}$  indicate the endothermic nature of the adsorption process. Whilst, a decrease of Gibb's free energy ( $\Delta G^0$ ) with increasing temperature indicates the spontaneous nature of the adsorption process. The adsorbent can be regenerated upto  $82.2\%$  with dilute acid and could be further utilized for removal of lead from contaminated water.

*Keywords:*

- A. Nanoparticles
- B. Chemical synthesis
- C. Electron microscopy
- D. Adsorption

## 1. Introduction:

Water pollution is one of the major problems faced by the world today. Heavy metals in water is a alarming threat to human as well as other animals because of their toxicity, accumulation in the food chain and prevalence in nature. Heavy metals (Pb, Cr, Cd, Hg, As etc.) in diverse forms constitute some of the major inorganic pollutants and have many harmful effects on humans including other animals and environment. Lead is one of the major polluting heavy element which leads a lot to increase physiological, biochemical, and behavioral dysfunctions, particularly in children, which is contaminated through the activity like plumbing fixtures, ceramics, glass, cable coverings, manufacture of storage batteries, paints and pigments, oil, solder, lead smelting and mining.<sup>1-4</sup> Among the top 20 hazardous substances as suggested by the Agency for Toxic Substances and Disease Registry (ATSDR) and United States Environmental Protection Agencies (USEPA), lead is among one of the major pollutants.<sup>5</sup> Though, the prescribed permissible limit of lead regulated by WHO is  $0.05 \text{ mgL}^{-1}$ , in industrial water it is found as high as  $200\text{--}500 \text{ mgL}^{-1}$ .<sup>6</sup> Hence, remedial measures are required to reduce the lead levels to desirable concentration for drinking and other domestic purposes.

With the emergence of nanoscience and technology in the last decade, research has been initiated to exploit the unusual and unique properties of nanomaterials for environmental remediation.<sup>7-9</sup> Among the various methods available for controlled synthesis, the “soft chemistry” routes, which are based on solution phase processes, are effective for the synthesis of nanostructured materials with well-controlled shapes, sizes, and structures.<sup>10-14</sup> There are some other techniques for synthesis of CuO nanoparticle but requires more cost, time as well as involvement of more reagents.<sup>15-17</sup>

In this regard, we have adopted a simple, cost effective and eco-friendly method to synthesize copper(II) oxide nanoparticle with rodlike symmetry. Thus synthesized nanoparticles have subsequently been used for adsorption of lead from contaminated water. We have also described adsorption of copper oxide varying different parameters like initial concentration, adsorbent dosage, pH and competing ions. Adsorption isotherm also described and found to follow multilayered adsorption isotherm.

## 2. Experimental

### 2.1 Materials

A round bottom flask, other glassware (borosil) along with reflux condenser and a heating mantle (REMI make, 200 W) were used as experimental set up for synthesizing the copper (II) oxide nanoparticles. Double distilled water was used throughout the experiments. All chemicals including Cupric Chloride (Merck, India), Sodium Hydroxide (Merck, India), Hydrochloric acid (Merck, India), capping solvent (PEG, MW 20000, SRL, Mumbai), lead nitrate (Merck, India), Potassium dichromate (Merck, India), acetone (Sigma Aldrich Pvt. Ltd, Bangalore) and ethanol (Bengal chemicals Pvt. Ltd., Kolkata) were analytical grade and used without further purification.

### 2.2 Synthesis

Copper (II) oxide nano has been synthesized following our reported earlier procedure with some modification in order to get uniform smaller particles.<sup>7</sup> Cupric Chloride ( $\text{CuCl}_2$ ), Sodium Hydroxide (NaOH) and capping solvent were mixed in 2:1:1 ratio with 200 mL ethanol in a round bottom flask fitted with reflux condenser. The mixture was refluxed for 10 h (around  $75^\circ\text{C}$ ) and allowed to cool to room temperature. Then the mixture was again refluxed for 5 hours. The product was washed with double distilled water and acetone repeatedly. The dark brown precipitate was centrifuged and

washed with ethanol, acetone and hot water respectively. Finally, the product was dried at room temperature and heated to 120°C vacuum oven in absence of air and cooled to normal temperature. Final product was used for adsorption experiments.

### 2.3 Adsorption experiments

Standard lead stock solution of 1000 mgL<sup>-1</sup> was prepared by dissolving 1.598 g of lead nitrate in 1L volumetric flask with double distilled water. 100 ml of each of working standard solution was taken in 250 ml conical flask and known weight of adsorbent material was added into it. The contents in the flask were shaken for 3 hours on a mechanical shaker (IKA 400 *ic* control) for different studies. The solution was centrifuged and the mother liquor was analyzed for residual contaminant concentration by Atomic Absorption Spectrometer. All adsorption experiments were conducted at room temperature (25°C ± 0.1 °C). Batch adsorption experiments were conducted to investigate the effect of various parameters like adsorbent dose, initial concentration, presence of interfering ions, pH etc.

The specific amount of contaminant adsorbed was calculated from:

$$Q_e = (C_0 - C_e) \times V / W \text{ ----- (1)}$$

Where  $Q_e$  is the adsorption capacity (mgg<sup>-1</sup>) in the solid at equilibrium;  $C_0$  and  $C_e$  the initial and equilibrium concentrations of metals/contaminant (mgL<sup>-1</sup>) respectively;  $V$  the volume of the aqueous solution;  $W$  is the mass (g) of adsorbent used in the experiments.<sup>18</sup> The effect of solution pH on lead removal were studied by adjusting the pH of the solution either by using 0.1N HCl or 0.1N NaOH. In slightly acidic as well as basic pH, copper oxide nanoparticle is stable and hence adsorption studies were carried out over the pH ranges of 5–11. The effects of the presence of competing ions such as calcium, sodium, hydroxide, chloride and iodide were studied at optimum experimental conditions (adsorbent dose 1gL<sup>-1</sup>, agitation speed 175 rpm,

temperature 25<sup>0</sup>C, contact time 3hrs). The experiment for reusability of used copper oxide nano was also performed. For this study, a certain amount of metal solution from working standard solution (200 and 500  $\mu\text{gL}^{-1}$ ) was initially allowed to adsorb on the nanoparticles at wide range of pH. After adsorption the solid was separated by filtration and dried in air. The dried adsorbent was repeatedly subjected to the contaminant/metals removal/adsorption experiments in order to examine the extent of reusability.

## 2.4 Characterization

Phase analysis of copper (II) nanoparticles was carried out using a X-ray diffractometer (PW 1710, Philips, Holland) with Co K $\alpha$  radiation ( $\lambda = 0.179$  nm) with a scanning rate of 3<sup>0</sup> per min. The morphology of the nanoparticles was studied by Field Emission Scanning Electron Microscope (FESEM) instrument (Supra 40, Carl Zeiss) at an accelerating voltage of 20 KV. The particle size of copper (II) nanoparticles was measured using a Transmission Electron Microscope (TEM) (CM 200, Phillips) at an acceleration voltage of 200 KV and digital images were taken on a Gatan multipole Charge Coupled Device (CCD) camera. Energy Dispersive X-ray (EDX) analysis of the sample was carried out on an Oxford Instrument INCA attached to the FESEM. Fourier Transform Infrared Spectroscopy (LR 64912C, Perkin Elmer) was used to analyze the different functional groups of the adsorbent through KBr pellet method. A BET surface area analyzer (Quantachrome NovaWin) was used to measure nitrogen adsorption isotherm at 77 K. Atomic Absorption Spectrometer studies were performed on Model: AA 7000, LabIndia Pvt. Ltd.

## 3. Results and Discussions

Figure 1 shows the typical X-ray diffraction (XRD) profile in the  $2\theta$  range of 20<sup>0</sup> to 70<sup>0</sup> of the synthesized copper(II) oxide, show the presence of the different characteristics peaks and

could be indexed on the basis of orthorhombic copper(II) oxide (JCPDS card no. 801268). It was matched from JCPDS file that the material is  $\text{Cu}_2\text{Cl}(\text{OH})_2$ .

Transmission electron microscopy (TEM) (Fig. 2a) shows that the nanorod is formed with diameter  $\sim 50$  nm. Figure 2b clearly reveals lattice picture with approx distance between two planes. Such a growth of nanorods in ethanol medium is not unusual and has already been observed in earlier reports.<sup>19-20</sup> Thus, for the present case, in all probability, ethanol acts as a soft template which facilitates the one dimensional growth of CuO nanorods.

The surface morphologies of copper(II) oxide nanorod before and after adsorption of lead from water were determined by FESEM images (Fig. 3a and Fig. 3b). Figure 4 revealed the presence of lead including other elements of CuO nano, indicating that adsorbent was capable to remove lead from water. The specific surface area of the CuO nanoparticle determined from BET surface area analyzer was  $52.57 \text{ m}^2\text{g}^{-1}$ .

FTIR spectroscopy is a useful tool to identify functional groups in a molecule, as each specific chemical bond often has a unique energy absorption band, and can obtain structural and bond information on a complex to study the strength and type of bonding.<sup>21</sup> Figure 5 represents FTIR spectra of the freshly prepared cupric oxide samples materials. The band at  $2933 \text{ cm}^{-1}$  and  $3432 \text{ cm}^{-1}$  belongs to the symmetric and asymmetric stretching vibration of O-H bond respectively. The presence of bands at  $523 \text{ cm}^{-1}$  and  $1011 \text{ cm}^{-1}$  indicates different modes of bending vibration of Cu-O bond. Appearance of peaks at  $1639 \text{ cm}^{-1}$  indicated stretching vibration of Cu-O bond of copper(II) oxide nanoparticle.

### 3.1 Effect of sorbent dosage

The effect of adsorbent (CuO nano) dosage on the adsorption of Pb(II) ion was studied using different dosage in the range,  $0.1\text{-}4 \text{ gL}^{-1}$ . The percentage removal of lead with different adsorbent

dosage is shown in Figure 6. The percentage removal of lead is significantly increased with sorbent dosage, which is because of increase in the number of active sites as the dosage increases.<sup>22</sup> It was observed that adsorption remains constant after  $1 \text{ gL}^{-1}$  of adsorbent dosage. Hence in all the subsequent experiments  $1.0 \text{ gL}^{-1}$  of adsorbent was fixed as the optimum dosage which could give reasonably good lead removal efficiency. Compared to other metal oxide, nano copper oxide is found to have better efficacy towards removal of lead from water.<sup>23-24</sup>

### 3.2 Effect of contact time

Figure 7 showed that the rapid adsorption of lead took place within 90 minutes. Thereafter, the process slows down and almost reached equilibrium within 180 minutes. No further appreciable adsorption takes (by less than 1%), place an increase in contact time up to 9 hrs, indicating that complete adsorption occurred within 3 hours. Thus, further adsorption experiments were conducted during 3 hours.<sup>25-26</sup>

### 3.3 Effect of initial concentration of adsorbate

To study the effect of initial concentration of lead ions on the extent of adsorption, dose of  $1 \text{ gL}^{-1}$  adsorbent dispersed in 2000 ppb of lead solution for contact time of 3 h and the findings are displayed in Figure 8. It has been observed that initially the rate of adsorption is fast and later it decreases with increase in concentration of lead. With increase in lead concentration, competition for the active adsorption sites increases and the adsorption process slows down.<sup>27</sup>

### 3.4 Influence of pH and mechanism of sorption

Influence of pH on Pb(II) adsorption by CuO were investigated and the data are shown in Fig. 9. From the Figure it is clear that Pb(II) adsorption by CuO nanorods is sensitive to pH variations.

However, for practical environmental application, the pH value of 8.3 has been taken as the experimental value as pH of drinking water should be within 6.5-8.5 (WHO/USEPA/BIS guidelines). In order to better assess the Pb(II) binding ability of adsorbents at various pH, the coefficient of distribution ( $K_d$ ) value has been determined using the following mathematical expression.

$$q = K_d C_e \text{ ----- (2)}$$

The  $K_d$  values thus obtained are plotted as a function of pH and the finds are shown in Fig. 10. It is important to mention here that higher the  $K_d$  value, better is the binding ability of the target pollutant.<sup>28</sup> In general, the  $K_d$  values in the range of  $10^3 \text{ mlg}^{-1}$  are considered good, and those above  $10^4 \text{ mlg}^{-1}$  are outstanding.<sup>29</sup> From the results (Fig. 10) it is clear that CuO nanorods are outstanding adsorbents in removing Pb(II) ions from aqueous solution. It is also observed that  $K_d$  vs pH plots of nano-CuO sharply increases with increase in pH indicating more sensitive nature of CuO to pH.

The extent of adsorption reportedly varies the solubility of the target metal. Therefore, it is important to know that whether Pb(II) removal at a particular pH has happened through lead hydroxide formation or adsorption of divalent lead ion. Following equations are used to calculate the pH at which lead hydroxide starts to form.<sup>30</sup>



$$\text{pH} = 14 - \log \frac{\sqrt{\text{Pb}^{2+}}}{\sqrt{K_{sp}}} \text{ ----- (4)}$$

$$K_{sp} = [\text{Pb}^{2+}] [\text{OH}^-]^2 \text{ ----- (5)}$$

where  $K_{sp}$  is the solubility product of lead hydroxide which is  $1 \times 10^{-16}$  at  $25^\circ\text{C}$ <sup>31</sup> and the  $[\text{Pb}^{2+}]_{\text{initial}} = 0.241 \mu\text{M}$  ( $500 \mu\text{gL}^{-1}$ ). Hence the pH at which  $\text{Pb(OH)}_2$  starts forming is calculated

~ 9.3 which rules out the precipitation of  $\text{Pb}(\text{OH})_2$  as the reason for  $\text{Pb}(\text{II})$  removal in our case ( $\text{pH} < 9.3$ ).

The effect of pH on the efficiency of sorbent was studied at different pH from 2 to 11 by keeping other experimental parameters constant (adsorbent dose  $1 \text{ gL}^{-1}$ , contact time 3hrs, RT) and shown in Figure 9. The percentage of lead removal was found more than 90 % at basic pH (9.0) whereas it was less than 75% at acidic pH (4.1). The variation in uptake with respect to the initial solution pH can be explained on the basis of ZPC of the adsorbent. To determine Zero Point Charge (ZPC) of nano-CuO, a plot made with initial pH of working lead solution vs final solution and shown in Figure 11 which shows that nano-CuO is neutral at pH 7.25 (=ZPC). Moreover, the maximum sorption capacity of the sorbent is found to be  $3.31 \text{ mgg}^{-1}$  at  $25^\circ\text{C}$ . Adsorption of lead has been also studied taking activated carbon and it has been found that maximum adsorption capacity is  $1.86 \text{ mgg}^{-1}$ . Meikap et. Al<sup>32</sup> also showed that activated carbon can be used as adsorbent for removal of lead with maximum adsorption capacity  $2 \text{ mgg}^{-1}$ .

When the adsorption system (lead solution/ copper oxide nanoparticle) was operated at  $7.25 < \text{pH} < 9.30$ , the reaction sites became negatively charged and contaminants with positive charge like lead are well adsorbed onto adsorbent. However, below  $\text{pH} = 7$ , adsorption decreased as there is slight repulsion between positively charged cation as well as that from adsorbent surface. Thus, the mechanism of lead removal by adsorption of copper oxide nanoparticle follows mainly physical rather than chemical as evident from enthalpy ( $\Delta H^0$ ) calculation.

### 3.5 Influence of competing anions

The contaminated drinking water may contain several common other anions, viz.,  $\text{OH}^-$ ,  $\text{Ca}^{2+}$ ,  $\text{Na}^+$  and  $\text{I}^-$  which could compete with lead ions during sorption process. Therefore, the

adsorption was studied in the presence of diverse ions with varying initial concentrations of these ions keeping the  $[\text{Pb}^{2+}]_{\text{initial}}$  as 200 and 500 ppb at RT.<sup>33</sup> Other experimental conditions *e.g.* agitation speed 175 rpm, temperature 25<sup>0</sup>C and contact time of 3 hrs are being kept constant and findings are displayed in Figure 10. It has been observed that with the increase in the concentration of these anions, removal of lead by the nanoparticle decreases which may be due to a competition among them for the sites on the sorbent surfaces, which in turn is decided by the concentration, charge and size of the anions.<sup>34</sup> Figure 10 also indicates that the presence of competing anions like hydroxide ion has a significant effect on lead adsorption followed by calcium. The percentage of lead removal decreased sharply after 0.01 mM concentration of hydroxide (OH<sup>-</sup>) ion with both concentration of lead solution and adsorption goes below 60% in the presence of hydroxide ion at 1mM. Thus, at basic pH, the nanoparticle possesses higher affinity towards the hydroxide ion compared to lead. Adsorption of lead decreases profoundly in presence of the calcium ion although calcium ion is of almost same size and charge due to competing ion effect. However, the concentrations of competing anions in this study were far higher than those likely to be encountered in groundwater. Thus, from these observations it can be concluded that copper oxide nanoparticles are able to remove lead from drinking water over a broad range of pH even at exceptionally high concentrations of the competing anions.

### 3.6 Temperature effect and thermodynamic study:

It is observed that with increase in temperature the lead adsorption percentage was also found to be increased, indicating the endothermic behavior of adsorption. In addition, the temperature dependence of adsorption and its thermodynamic have been studied at three different temperature viz. 298K, 308K, 318K and the thermodynamic parameters viz. Gibb's free energy

( $\Delta G^0$ ), entropy ( $\Delta S^0$ ) and enthalpy ( $\Delta H^0$ ) changes for the adsorption process were determined by following equations.<sup>35</sup>

$$\Delta G^0 = \Delta H^0 - T\Delta S^0 \quad \text{-----} \quad (6)$$

$$\log \left( \frac{q_e m}{C_e} \right) = \frac{\Delta S^0}{2.303R} + \frac{-\Delta H^0}{2.303RT} \quad \text{-----} \quad (7a)$$

For unit adsorbent mass, Eq. (7a) became

$$\log \left( \frac{q_e}{C_e} \right) = \frac{\Delta S^0}{2.303R} + \frac{-\Delta H^0}{2.303RT} \quad \text{-----} \quad (7b)$$

where  $q_e$  is the amount of lead adsorbed per unit mass of adsorbent ( $\mu\text{g/g}$ ),  $C_e$  is the equilibrium concentration ( $\mu\text{g/L}$ ),  $m$  is the adsorbent mass ( $\text{g/L}$ ) and  $T$  is temperature in Kelvin.  $q_e/C_e$  is called the adsorption affinity. The values of Gibb's free energy ( $\Delta G^0$ ) was calculated by knowing the enthalpy of adsorption ( $\Delta H^0$ ) (from plot of  $\log(q_e/C_e)$  versus  $1/T$ ) and entropy of adsorption ( $\Delta S^0$ ). From these,  $\Delta G^0$  is determined applying Eq. (5). Thus obtained thermodynamic parameters are summarized in Table 1 corresponding to solution  $[\text{Pb}_{2+}]_{\text{initial}} = 500 \mu\text{g/L}$ . The +ve  $\Delta H^0$  and -ve  $\Delta G^0$  values clearly indicates the endothermic behavior of adsorption and spontaneous nature of the adsorption process respectively<sup>36</sup>. The low value of  $\Delta S^0$  indicates that no remarkable change in entropy occurred during the adsorption process<sup>37</sup>. However, +ve  $\Delta S^0$  value indicates the increased randomness at the solid-solution interface during adsorption. The value of  $\Delta H^0$  ( $37.77 \text{ kJmol}^{-1}$ ) indicates that the adsorption process is a physico-chemical adsorption process rather than a pure physical or chemical adsorption as heats of chemisorptions generally falls into a range of  $80\text{--}200 \text{ kJmol}^{-1}$ .

### 3.7 Adsorption isotherms

The adsorption isotherms are generally used to describe how adsorbate interacts with adsorbent at equilibrium and therefore it is critical in optimising the use of adsorbents. Two different isotherms have been adopted to understand the mechanism of adsorption for the removal of lead. Theoretical plots of each isotherm were tested for their correlation with the experimental results. Figure 13 showed the comparison of different isotherms studied at 25°C.

The adsorption isotherm can show adsorption capacity at different equilibrium concentration. The adsorption process could be described by the Langmuir and Freundlich isotherms. Fig. 13 shows isotherm for Pb ions on the CuO nanomaterials at 25°C. The Langmuir equation assumes that no further adsorption can take place at that site if a Pb ion occupies a site. The Langmuir equation<sup>38</sup> is expressed as follows:

$$q_e = \frac{q_m b C_e}{1 + b C_e} \text{-----} (8)$$

Where,  $q_e$  is the equilibrium quantity adsorbed ( $\text{mgg}^{-1}$ ),  $q_m$  is the maximum capacity of monomer adsorption ( $\text{mgg}^{-1}$ ),  $C_e$  the equilibrium concentration of remaining Pb ions in solution ( $\text{mgL}^{-1}$ ),  $b$  the adsorption equilibrium constant ( $\text{Lmg}^{-1}$ ) related to the energy of adsorption. In order to predict the adsorption efficiency of the process, the dimensionless equilibrium parameter ( $R_L$ ) was determined using the following equation:

$$R_L = \left( \frac{1}{1 + b C_0} \right) \text{-----} (9)$$

Where,  $C_0$  ( $\text{mg/L}$ ) is the initial concentration of working lead solution. The  $R_L$  value calculated was found to be lying between 0 and 1 which indicated favorable adsorption for all initial lead solution concentrations.

The Freundlich equation is an empirical equation and has the following form:<sup>39</sup>

$$q_e = K_f C_e^{1/n} \text{-----} (10)$$

where,  $K_f$  ( $\text{mg}^{1-1/n} \text{L}^{1/n} \text{g}^{-1}$ ) is Freundlich constant indicative of the relative adsorption capacity of the CuO nanoparticles and  $n$  is the empirical parameter representing adsorption intensity of the CuO nanoparticles.

The maximum adsorption capacity was found to be 3.31 mg of Pb ions adsorbed per gram of CuO nano particles with calculated adsorption equilibrium constant,  $b$  value of 1.96  $\text{L mg}^{-1}$ . The equilibrium adsorption data fitted better to Freundlich isotherm ( $R^2=0.9510$ ) with root mean square error (RMSE) value being 0.0946 as compare to Langmuir isotherm ( $R^2=0.9431$ ) with RMSE value being 0.1144). The value of  $K_f$  calculated was found to be  $1.80 \text{ mg}^{1-1/n} \text{L}^{1/n} \text{g}^{-1}$

### 3.8 Lead desorption study

The exhausted copper oxide nanoparticles were regenerated with eluents like dilute HCl and dilute NaOH.<sup>40</sup> All the regeneration experiments were carried out at room temperature. Desorption efficiency of the nanoparticles was studied using 0.2M and 0.5M HCl as well as same concentration of NaOH as eluents. From Table 1 it is evident that out of the two eluents, HCl had been identified as the best eluent as it had 82.4% desorption efficiency whereas NaOH showed a maximum of 72% desorption efficiency.

## 4. Conclusions

CuO nanoparticle prepared through easy and soft chemistry route are found to be excellent candidates for removing Pb(II) from aqueous solutions. As far as practical applicability is concerned, CuO is more promising and is effective over a wide range of pH in presence of other

competing/interfering ions. Reduced sensitivity to pH makes this adsorbent more attractive for cleaning up industrial effluents, especially effluents having low pH. The +ve  $\Delta H^0$  (37.77 kJmol<sup>-1</sup>) and -ve  $\Delta G^0$  values clearly indicates the endothermic behavior of adsorption and spontaneous nature of the adsorption process respectively. The adsorption process is a physico-chemical adsorption process rather than a pure physical or chemical adsorption with +ve  $\Delta S^0$  value indicating the increased randomness at the solid-solution interface during adsorption. Equilibrium sorption data shows the sorption is multilayered on the heterogeneous surface of the nano adsorbent with maximum adsorption efficiency of the sorbent is 3.31 mgg<sup>-1</sup> for lead at room temperature. Regeneration study reveals that the as-synthesized adsorbent can be regained and used multiple times by treating the spent adsorbent by an acid like HCl and alkali like NaOH.

**References:**

1. E.C. Banks, L.E. Ferretti and D.W. Shucard, *Neurotoxicology*, 1997, **18**, 237–281.
2. S. Tunali, T. Akar, A.S. Ozcan, I. Kiran and A. Ozcan, *Sep. Purif. Technol.*, 2006, **47(3)**, 105–112.
3. K. Conrad and H.C.B. Hansen, *Bioresour. Technol.*, 2007, **98**, 89–97.
4. E. Eren, B. Afsin and Y. Onal, *J. Hazard. Mater.*, 2009, **161**, 677–685.
5. J J.Moros, I. Llorca, M.L. Cervera, A. Pastor, S. Garrigues and M. de la Guardia, *Anal. Chim. Acta*, 2008, **613**, 196–206.
6. A.S. Özcan, Ö. Gök and A. Özcan, *J. Hazard. Mater.*, 2009, **161**, 499–509.
7. A. Goswami, P. K. Raul and M. K. Purkait, *Chem. Eng. Res. and Design*, 2012, **90**, 1387-1396.
8. Prasanta K Raul, Rashmi R Devi, Iohborlang M Umlong, Saumen Banerjee, Lokendra Singh and Mihir Purkait, *J. Nanosc. and Nanotech.*, 2012, **12**, 3922-3930.
9. Suman Thakur, Gautam Das, Prasanta Kumar Raul and Niranjana Karak, *J. Phys. Chem. C*, 2013, **117**, 7636–7642.
10. B. I. Kharisov, H.V. Rasika Dias and O.V. Kharissova, *RSC Adv.*, 2012,**2**, 9325-935;
11. Mandakini Biswal, Kirti Bhardwaj, Pradeep K. Singh, Pooja Singh, Prasad Yadav, Asmita Prabhune, Chandrashekhara Rodea and Satishchandra Ogale, *RSC Adv.*, 2013, **3**, 2288-2295.
12. Jing Zhang, Guilong Zhang, Min Wang, Kang Zheng, Dongqing Cai and Zhengyan Wu, *Nanoscale*, 2013,**5**, 9917-9923
13. B.L. Cushing, V.L. Kolesnichenko and C.J. O'Connor, *Chem. Rev.*, 2004, **104**, 3893–3946.
14. H. Chen, J. He, C. Zhang and H. He, *J. Phys. Chem.*, 2007, **111**, 18033–18038.
15. Shaodong Sun, Xiaozhe Zhang, Yuexia Sun, Shengchun Yang, Xiaoping Song and Zhimao Yang, *Phys. Chem. Chem. Phys.*, 2013,**15**, 10904-10913.
16. M. Ashraf Shah and M. S. Al-Farah, *Materials Sciences and Application*, 2011, **2**, 977-980.

17. Linlin Wang, Wei Cheng, Huaxu Gong, Caihua Wang, Dake Wang, Kaibin Tang and Yitai Qian, *J. Mater. Chem.*, 2012, **22**, 11297-11302
18. O. Abdelwahab, *Egypt. J. of Aqua. Res.*, 2007, **33**, 125-143.
19. R.P. Jia, Y.Q. Zhang, *J. of Nanoparticle Res.*, 2010, **12**, 2717-2721.
20. M.Y. Tsvetko, B.N. Khlebtso, V.A. Khanadee, V.N. Bagratashvil, P.S. Timashe, M.I. Samoylovic and N.G. Khlebtso, *Nanoscale Res. Letters* 2013, **8**, 250.
21. N. Li and R. Bai, *Ind. Eng. Chem. Res.*, 2005, **44**, 6692–6700.
22. S. Mellah and Chegrouche, *Water Res.*, 1997, **31**, 621-629.
23. Hua M, Zhang S, Pan B, Zhang W, Lv L and Zhang Q, *J. Haz. Mater.*, 2012, **211**, 317-331.
24. T. S. Sreeprasad, S. M. Maliyekkal, K. P. Lisha and T. Pradeep, *J. Haz. Mater.*, 2011, **186**, 921-931.
25. A. Ozer and D. Ozer, *J. Haz. Mater.*, 2003, **100**, 219-229.
26. A. Sari, M. Tuzen, Department of Chemistry, Gaziosmanpasa University, 60250 Tokat, Turkey
27. T.K. Naiya, A.K. Bhattacharya, S. Mandal, S.K. Das, *J. of Haz. Mater.*, 2009, 163, 1254–1264.
28. N. Sharma, K. Kaur, S. Kaur, *J. of Haz. Mater.*, 2009, 163, 1338–1344.
29. W. Yantasee, C.L. Warner, T. Sangvanich, R.S. Addleman, T.G. Carter, R.J. Wiacek, G.E. Fryxell, C. Timchalk and M.G. Warner, *Environ. Sci. Technol.*, 2007, **41**, 5114–5119.
30. Y. AlDegsa, M.A.M. Khraisheh and M.F. Tutunjib, *Water Res.*, 2001, **35**, 3724–3728.
31. L. Pauling, A book on General Chemistry, Dover Publishing, 1970, p. 456
32. C. P. Dwivedi, J.N. Sahu, C.R. Mohanty, B. Raj Mohan and B.C. Meikap, *J. Haz. Mater.*, 2008, **156**, 596–603.
33. Mya Mya Khin, A.S. Nair, V. Jagadeesh Babu, Rajendiran Murugana and Seeram Ramakrishna, *Energy Environ. Sci.*, 2012, **5**, 8075-8109.

34. E. Erdem, N. Karapinar, R. Donat, *J. of Colloid and Interface Sci.*, 2004, 280, 309–314.
35. C. Namasivayam and D. Kavitha, *Dyes and Pigments*, 2002, **54**, 47–58.
36. C. Xiong, C. Yao, L. Wang, Jiajun, *Hydrometallurgy*, 2009, **98**, 318–324.
37. L. Zeng, *Water Qual. Res. J. Canada*, 2004, **39**, 267–275.
38. I. Langmuir, *J. Am. Chem. Soc.*, 1918, **40**, 1361- 1403.
39. H.Z. Freundlich, *J. Phys. Chem.*, 1906, **57A**, 385- 470.
40. N. Viswanathan, C.S. Sundaram and S. Meenakshi, *J. Hazard. Mater.*, 2009, **161**, 423–430.

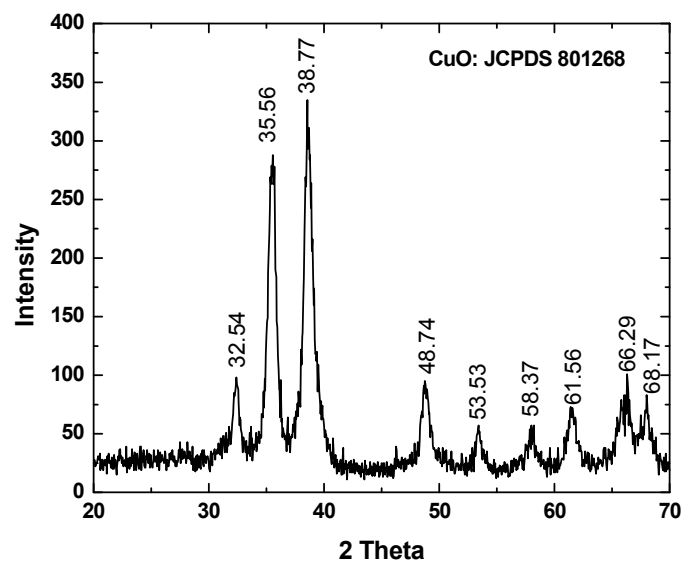


**Fig. 1.** XRD of Copper oxide nanoparticles.

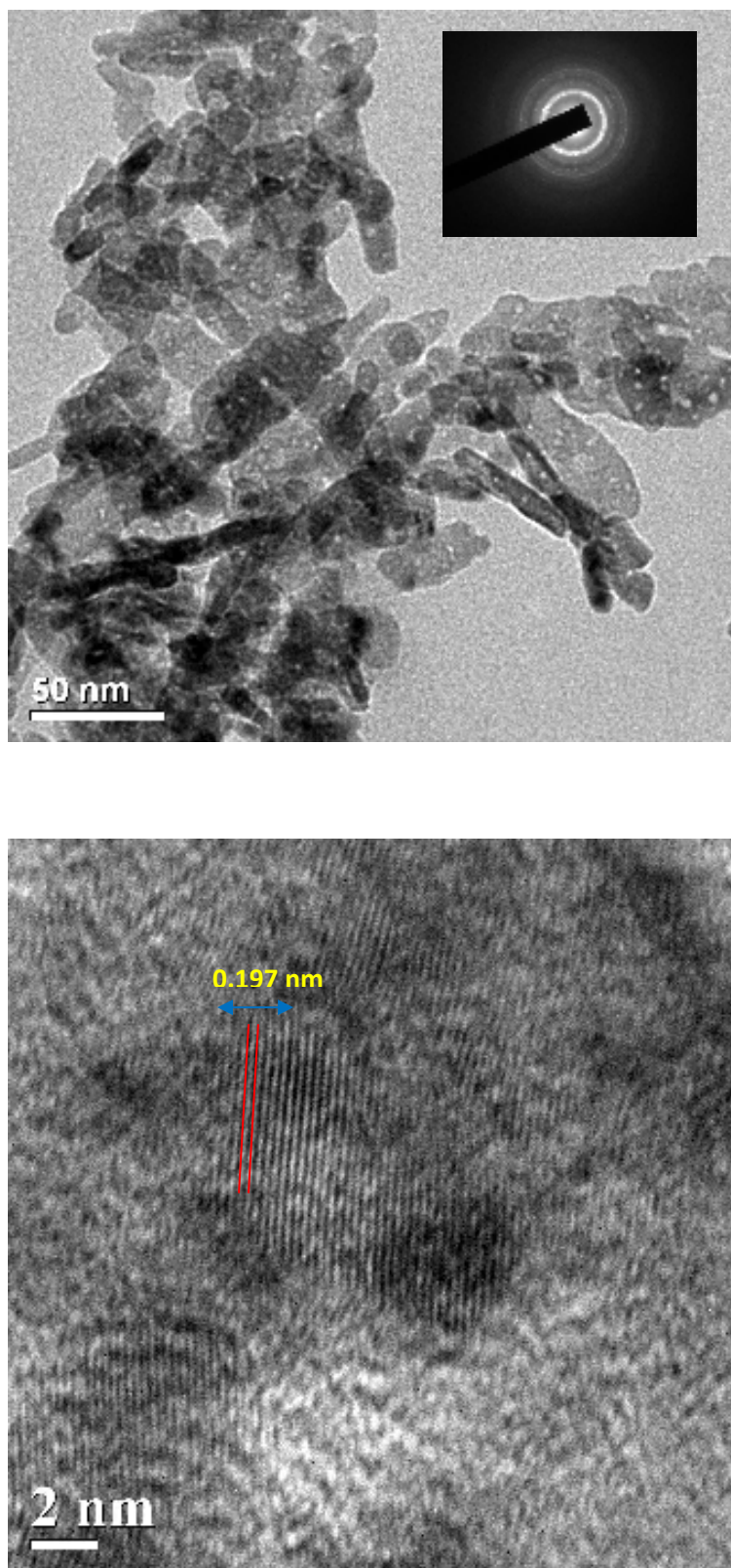


**Fig.2. a)** TEM and SAED image of copper(II) oxide nanoparticles **b)** HRTEM image

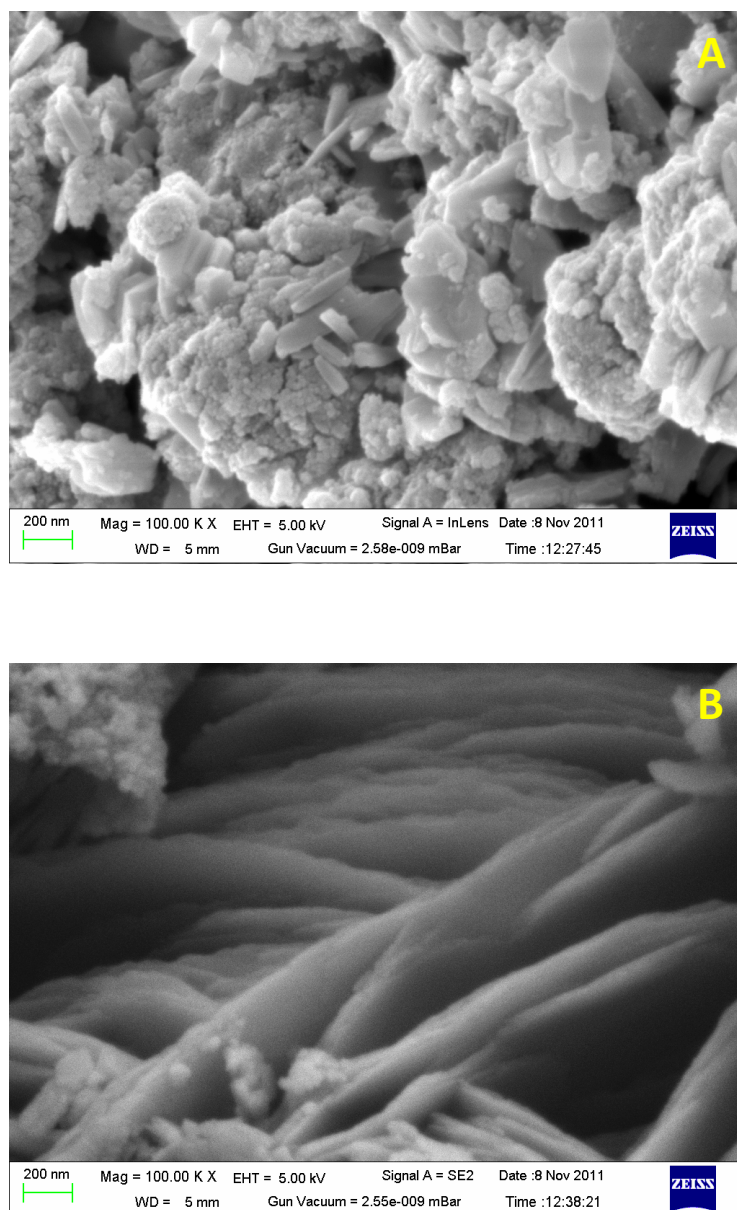


**Fig. 3.** FESEM of copper oxide nanoparticles before (A) and after (B) adsorption of lead

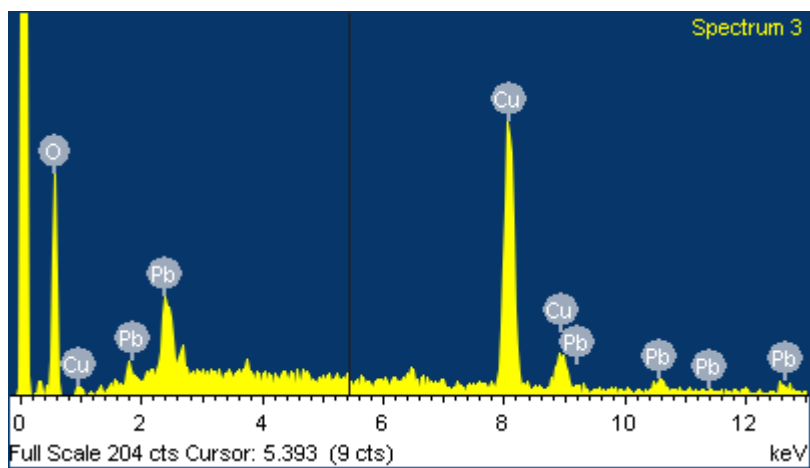


**Fig. 4.** EDX analysis of Copper Oxide nanoparticles after adsorption of lead

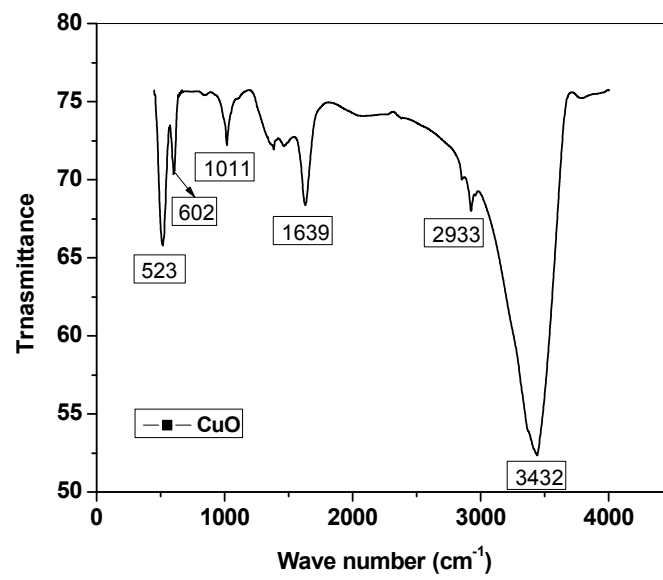


Fig. 5. FTIR of Copper Oxide nanoparticle

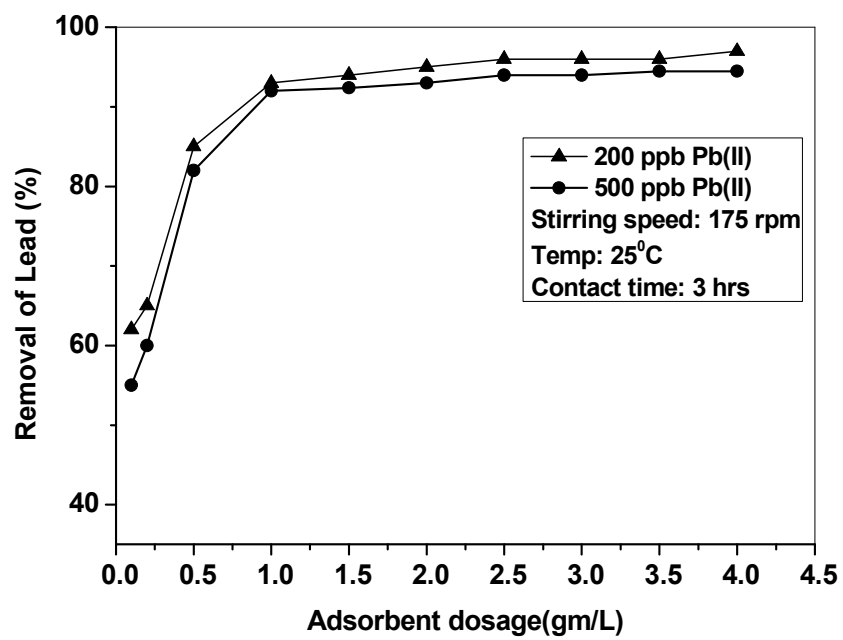


Fig. 6. Variation of adsorbent dose on the removal of Lead

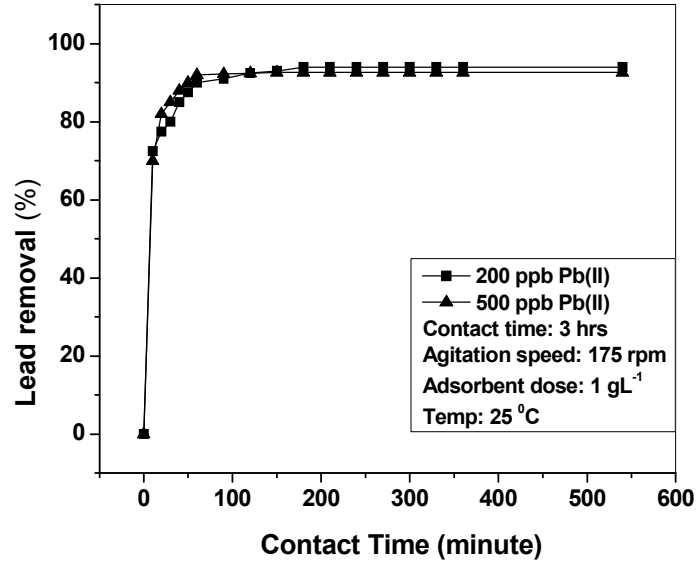
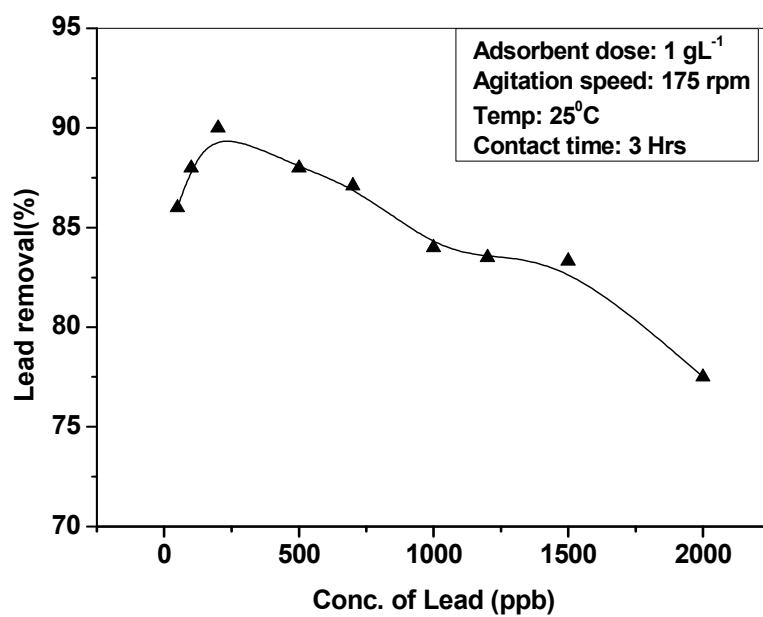
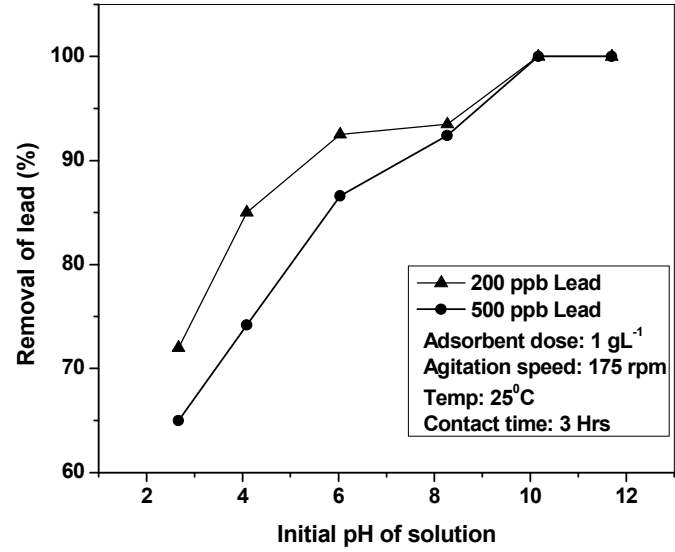


Fig. 7. Removal of Lead Vs contact time of agitation



**Fig. 8.** Variation of initial conc. of lead on the removal of Lead



**Fig.9.** Removal of lead Vs initial pH of the working solution

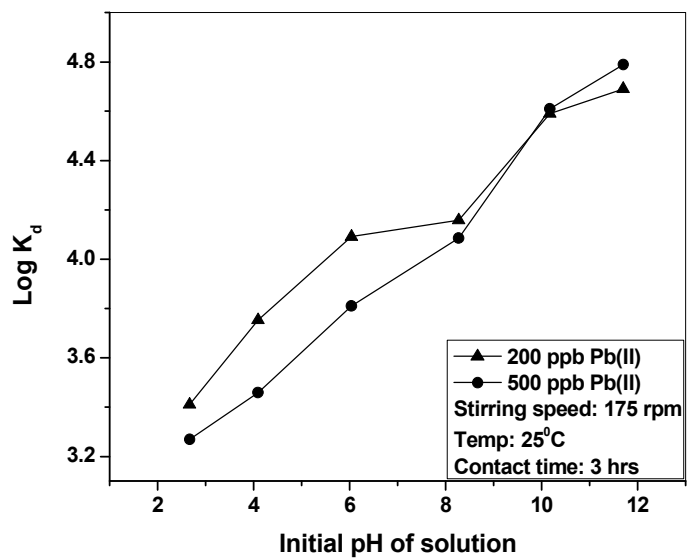


**Fig. 10.** Plot of Log  $K_d$  Vs initial pH of lead solution

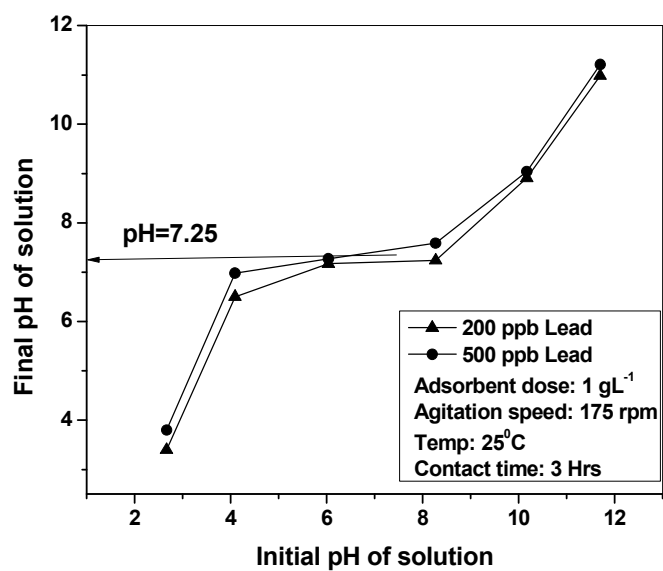
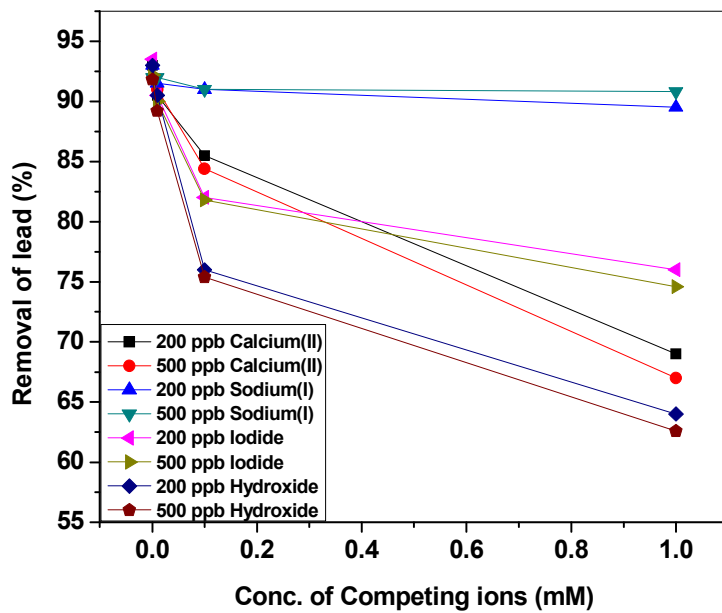


Fig. 11. Plot of Final pH with Initial pH of lead solution



**Fig.12.** Effect of competing ions on removal of lead

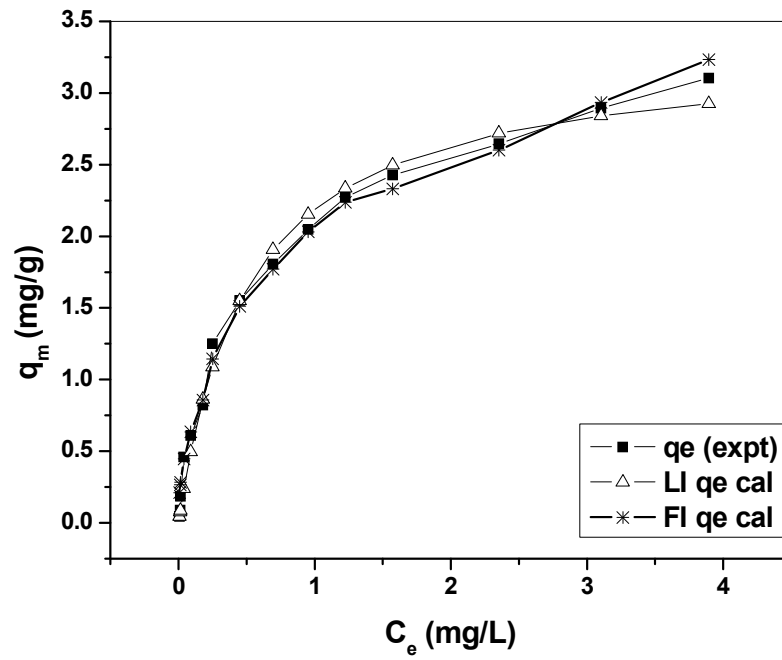


Fig.13. Equilibrium isotherm model for lead adsorption.

**Table 1:** Thermodynamic parameters for lead adsorption on CuO nanorods

Temperature(K)	$\Delta H^0$ (kJmol <sup>-1</sup> )	$\Delta S^0$ (kJmol <sup>-1</sup> K <sup>-1</sup> )	$\Delta G^0$ (kJmol <sup>-1</sup> )
298	-	-	-36.76
308	37.77	0.25	-39.23
318	-	-	-41.73

**Table 2:** Regeneration study (adsorbent dosage: 1 gL<sup>-1</sup>)

Initial conc of pb(II) mgL <sup>-1</sup>	Conc. of adsorbed lead (mgL <sup>-1</sup> )	Eluent used	Conc of eluent (M)	Conc of pb(II) in eluent after treatment (mgL <sup>-1</sup> )	Regeneracy of Lead (%)
200	196	NaOH	0.2	120	61.22
200	196	NaOH	0.5	140	71.43
200	196	HCl	0.2	160	<b>81.63</b>
200	196	HCl	0.5	194	<b>Soluble</b>
500	490	NaOH	0.2	320	65.30
500	490	NaOH	0.5	360	73.47
500	490	HCl	0.2	412	<b>84.10</b>
500	490	HCl	0.5	488	<b>soluble</b>